Available online at www.sciencedirect.com

SciVerse ScienceDirect

Physics Procedia 32 (2012) 144 – 151

Physics Procedia

18th International Vacuum Congress (IVC-18)

Transport properties of amorphous $Ge_{20}Te_{80-x}Bi_x$ glassy alloys

Ambika Sharma[a] and P.B. Barman[b]

[a]Department of Applied Sciencs and Humanities,ITM University Gurgaon Haryana (122017) India
[b]Department of Physics, Jaypee University of Information Technology, Waknaghat, Solan, H.P. (173215) India

Abstract

Bulk samples of $Ge_{20}Te_{80-x}Bi_x$ (x = 0, 1.5, 2.5, 5.0) glassy alloy are prepared by melt quenching technique. Differential scanning calorimetric (DSC) technique has been applied to determine the thermal properties of Te-rich $Ge_{20}Te_{80-x}Bi_x$ glassy alloys in the glass transition and crystallization regions. The glass transition temperature (T_g) as well as crystallization temperature (T_c) is found to increase with increasing Bi content. This behavior is explained on the basis of coordination number m and deviation from stoichiometry, R values. From the temperature dependent dc conductivity measurements, the activation energy (ΔE) and the pre-exponential factor (σ_0) are calculated for each glassy alloy. Optical band gap is calculated using Tauc extrapolation method and is found to decrease with increase in Bi content. It has been observed that the value of ΔE is less than half of optical band gap (E_g) indicating that the Fermi level is not located near the centre of gap.

Keywords: Glass Transition Temperature, Dark conductivity, Optical band gap

1. Introduction

Chalcogenide glasses have attracted the attention of many investigators due to their potential applications in IR optics, photonics device, reversible optical recording, memory switching, inorganic photo resists, antireflection coating, optical data storage, frequency doubling, optical limiter etc [1-8]. The interest in these materials arises particularly due to their ease of fabrication in the form of bulk and thin films. Furthermore, one can easily change the properties of these glasses by varying their chemical composition (synthesis regime). A typical chalcogenide has a relatively sharp optical absorption edge and single electrical activation energy. The Te based chalcogenide glasses are used for such applications because their infrared absorption edges are located in a wavelength region above 12 μm [9]. However, only few compositions such as Ge-Te and As-Te based glasses have been investigated as memory switching glasses [10-14]. It is supposed that amorphous $GeTe_2$ structure with fourfold coordination of Ge and two fold coordination of Te is most stable in the alloys containing less than 33 at.% of Ge. The existence of strong covalent bonding in a-Ge-Te has been proven by photoemission measurements in [15]. Moreover, the covalency in amorphous phase was shown to be stronger than in crystalline phase. From the experimental structure factors and pair correlation functions of Ge-Te alloys as investigated by I. Kaban et.al. [16], one may guess that amorphous Ge-Te alloys are a random mixture of Ge and Te atoms, and Ge-Te bonds are formed statistically when Ge is added. On the other hand, it can be supposed that Te- rich Ge-Te amorphous alloys are chemically ordered on the microlebel and some structural units with strong Ge-Te bonds are distributed among Te atoms. It was established that $Ge_{20}Te_{80}$ composition alloy shows single- stage amorphous-to- crystalline transformation due to simultaneous formation of Ge-Te and Te crystallites, whereas the alloy

1875-3892 © 2012 Published by Elsevier B.V. Selection and/or peer review under responsibility of Chinese Vacuum Society (CVS).
Open access under CC BY-NC-ND license. doi:10.1016/j.phpro.2012.03.532

containing 15 at.% Ge exhibits two-stage transformation due to segregation of Te and subsequent formation of GeTe crystallites. Obviously this difference in the crystallization of the Ge-Te alloys is explained by differences in their atomic structure. It is supposed that all Ge atoms in $Ge_{20}Te_{80}$ composition alloy are bonded with Te atoms with stiochiometry $GeTe_4$. On the other hand the alloy between $Ge_{20}Te_{80}$ and pure Te contain $GeTe_4$ tetrahedra as structural units and Te atoms distributed among them. For $Ge_{20}Te_{80}$ glassy alloy, elastic recovery of deformation is maximum [17]. $Ge_{20}Te_{80}$ composition glass network lies at the threshold of the mode change i.e. floppy to intermediate region having an average coordination number m = 2.4. According to constraint model and development theories [18, 19], by equating the number of operative constraints to the number of degrees of freedom, m of the most stable glass is shown to be of value 2.4. So the addition of third element in Ge–Te tetrahedral glassy network makes the glass an interesting material and new properties are expected. The addition of Bismuth (Bi) into $Ge_{20}Te_{80}$ system in an effective way controls its electrical, optical and physical properties as this will lead the system towards the intermediate region. The present paper deals with the thermal, optical and electrical properties of $Ge_{20}Te_{80-x}Bi_x$ glassy alloy. The corresponding change in the thermal parameters is related with the structural changes occurring in the system due to the variation in coordination number.

2. Experimental Details

Glassy alloys of the $Ge_{20}Te_{80-X}Bi_x$ (x = 0, 1.5, 2.5, 5.0) system have been prepared by the quenching technique as described elsewhere [20]. Thin films of the glassy alloys have been prepared by the vacuum evaporation technique, keeping the substrates at room temperature with a base pressure of ~ 2×10^{-5} mbar. The amorphous nature of the bulk samples and thin films was confirmed by the x-ray diffraction technique (Rigaku Geiger Flex 3KW Diffractometer using CuKα source) as no sharp peak was observed in the spectra. The compositions of evaporated films were measured by an electron microprobe analyzer (JEOL 8600 MX) on the different spots (size ~ 2μm) of the films. For the compositional analysis, the constitutional elements (Ge, Te and Bi) and the bulk original alloys, i.e. $Ge_{20}Te_{80-X}Bi_x$, were taken as reference samples. The compositions of a 2×2 cm^2 sample were found to be uniform within the measurement accuracy of about ±2%. Thermal behavior of the sample is recorded using Shimadzu DTG-60 system in order to get (T_g), (T_p) and (T_m) for the system. Predeposited thick indium electrodes on well-degassed Corning 7059 glass substrates have been used for the electrical contacts. A planar geometry of the film (length ~ 1.78 cm; electrode gap ~ 8×10^{-2} cm) is used for the electrical measurements. The dc conductivity measurements were carried out in the temperature range 300-363 K in a running vacuum of ~10^{-3} mbar. The current was measured by a digital picometer (Keithley, model 6487). The normal incidence transmittance and reflectance spectra in the spectral range 700–2400 nm of films were obtained by a double beam ultraviolet–visible–near infrared spectrophotometer (Perkin Elmer Lambda-750). All measurements were performed at room temperature (300 K).

3. Results and Discussion

3.1 Thermal studies

DTA curves of $Ge_{20}Te_{80-X}Bi_x$ (x = 0, 1.5, 2.5, 5.0) glassy alloy are shown in Fig. 1. It is clear that the value of glass transition temperature *(T_g)* as well as crystallization temperature *(T_c)* increases with increase in Bi content (Table 1). The effective increase in glass transition temperature is explained on the

basis of coordination number of the system which increases with the increase in Bi content. Coordination number in $Ge_{20}Te_{80-x}Bi_x$ system has been calculated using the relation

$$m = \frac{\alpha N_{Ge} + \beta N_{Te} + \gamma N_{Bi}}{\alpha + \beta + \gamma} \tag{1}$$

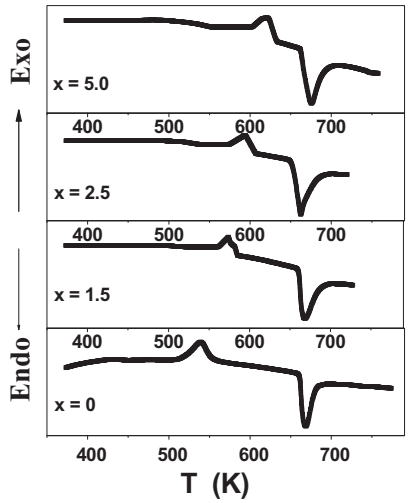

Fig. 1 Plot of DTA thermograms for $Ge_{20}Te_{80-X}Bi_x$ glassy alloy at 20 ˚C/min heating rate.

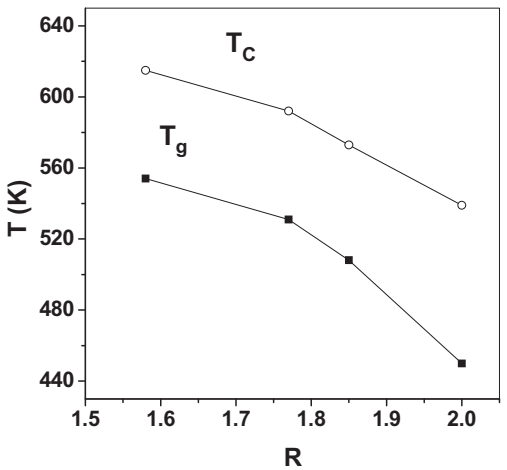

Fig. 2 Plot of $\left(T_g\right)$ and *(T_C)* vs. *R* for $Ge_{20}Te_{80-X}Bi_x$ glassy alloy

where α, β and γ are the at. % of Ge, Te and Bi, respectively, and N_{Ge}= 4, N_{Te}= 2 and N_{Bi} = 3 are their respective coordination numbers. The value of coordination number (m) values lie in range 2 to 2.5. The calculated values of m (listed in Table 1) indicate that its value increases with increase of Bi content. In chalcogenide based glasses T_g represents the temperature above which an amorphous matrix can attain various structural configurations and below which the matrix is frozen into a structure which cannot easily change to another structure. Therefore, it is reasonable to assume that T_g must be related to the structural changes and hence coordination number of the network. The glass transition temperature T_g of chalcogenide glasses shows coordination number dependence. It increases linearly with increase in coordination number and follows the relation [21]

$$\ln(T_g^{th}) = 1.6m + C \tag{2}$$

where C = 2.3. The theoretically calculated values of T_g^{th} are tabulated in table 1. The dependence of T_g and T_c on composition for the present glassy system is also explained on the basis of deviation of stoichiometry, R of the system. R is expressed by the ratio of covalent bonding possibilities of chalcogen atom to that of nonchalcogen atom. Values of R were found to be larger than unity for such glasses, which indicate chalcogen-rich materials and less than unity for the glass which shows chalcogen poor material. For $Ge_xTe_yBi_z$ system, the quantity R is defined by [22, 23]

$$R = \frac{yCN(Te)}{xCN(Ge) + zCN(Bi)} \tag{3}$$

where x, y and z are the atomic fractions of Ge, Te and Bi respectively. The threshold at R = 1 (the point of existence of only heteropolar bonds) is evident. For present investigating system the values of R are greater than 1 (see table 1) leading the system to chalcogen-rich region. Fig. 2 shows the variation of T_g and T_c with R-value. Consequently the increase in T_g and T_c with decrease in R- value can be interpreted as occurring due to the approaching of chemical threshold [24]. The thermal stability of the glass is generally measured by the difference $\Delta T = T_c - T_g$. For the present system, the value of ΔT is maximum for x = 0 (Table 1), indicating the maximum thermal stability at chemical threshold. The reduced glass transition temperature is calculated as $T_{rg} = T_g / T_m$ and its value is nearly equal to 2/3 for all the samples (Table 1).

Table 1. Values of T_g, T_c, T_m, ΔT, T_{rg}, m, R and T_g^{th} calculated from DTA thermograms at 10 K/min heating rate, for $Ge_{20}Te_{80-X}Bi_x$ system.

x	$T_g(K)$	$T_C(K)$	$T_m(K)$	ΔT (K)	T_{rg}	m	R	$T_g^{th}(K)$
0	450	539	667	89	0.45	2.40	2.00	267
1.5	508	573	669	65	0.59	2.42	1.85	270
2.5	531	592	665	61	0.66	2.43	1.77	273
5.0	554	615	674	61	0.70	2.45	1.58	279

3.2 Electrical and optical studies.

Fig. 3 shows the temperature dependence of dark conductivity (σ_d) for $Ge_{20}Te_{80-X}Bi_x$ thin films typically at 80 V. The plots of ln (σ_d) versus 1000/T are found to straight lines indicating that the conduction is through an activated process having single activation energy in the temperature range 300-360 K. In most of the chalcogenide glasses, σ_d can therefore be expressed by Arrhenius relation [25]

$$\sigma_d = \sigma_0 \exp\left(\frac{-\Delta E_d}{kT}\right) \tag{4}$$

Where σ_0 is the material related pre exponential factor, ΔE_d is the activation energy for dc conduction, *k* is the Boltzman constant and *T* is the temperature. The value of ΔE_d is estimated from the slope of ln (σ_d) versus 1000/T curves. The calculated values of ΔE_d , σ_d and σ_0 at room temperature are inserted in table 2. The composition dependent dark conductivity and activation energy is studied and it is observed that with the increase of Bi content conductivity increase and activation energy decreases. This behavior may be explained on the basis of Mott and Davis model. According to this model there can be three processes leading to conduction in amorphous semiconductors. At very low temperature conduction can occur by thermally assisted tunneling between states at the Fermi level. At higher temperature, charge carriers are excited into the localized states of the band tails; carriers in their localized states can take part in the electric charge transport only by hoping. At still higher temperature, carriers are excited across the mobility edges into the extended states. According to Mott and Davis [25] the value of σ_0 determines the process of conduction in amorphous semiconductors.

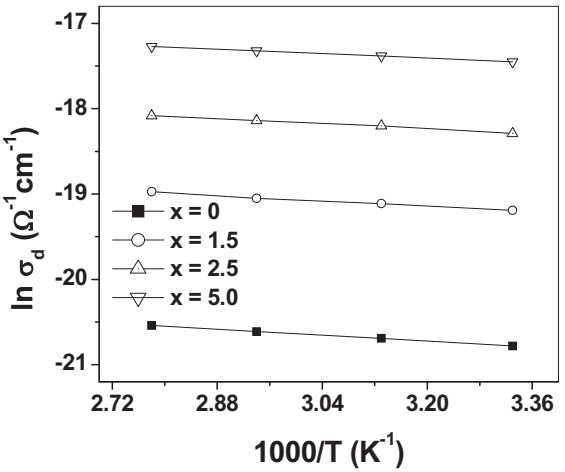

Fig. 3 Plot of ln (σ_d) vs. 1000/T for $Ge_{20}Te_{80-X}Bi_x$ thin films.

For very small value of σ_0 the conduction is through localized states, whereas if the value of σ_0 falls in the range 10^2 -10^3, the conduction is considered through extended states. In the present case the value σ_0 falls in range 10^2 -103, and therefore conduction is supposed to be through extended states. The variation of dc parameters with Bi for the investigated composition may also be explained by assuming that Bi atoms act as impurity centers in the mobility gap and induces structural changes in the network which may disturb the balance of charged defects and consequently change the electric conduction.
The optical absorption coefficient (α) is calculated from the transmission and reflection spectra using the relation [26]

$$\alpha = \frac{2.303}{d}\log\left(\frac{1-R}{T}\right) \tag{5}$$

where d is the film thickness (d ≈ 500 nm for all the samples with an uncertainty of ± 20%), T is the transmittance and R reflectance. α has been found to be of the order of 10^4 cm^{-1}. Optical band gap (E_g) has been determined according to the generally accepted 'non direct transition' model for amorphous semiconductors proposed by Tauc [27], which assumes that the densities of electron states in the valence and conduction bands near the band gap have a parabolic distribution. The relation is

$$\alpha h\nu = B(h\nu - E_g)^2 \tag{6}$$

where $B^{1/2}$ is so called Tauc slope. The graph between $(\alpha h\nu)^{1/2}$ and $h\nu$ for $Ge_{20}Te_{80-X}Bi_x$ films is shown in the Fig. 4. The intercept on energy axis provides the value of E_g..

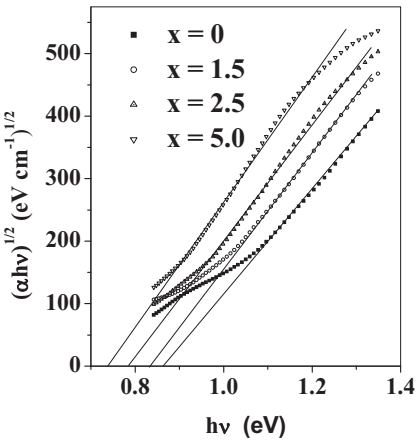

Fig. 4 Plot of $(\alpha h\nu)^{1/2}$ vs. $h\nu$ for $Ge_{20}Te_{80-X}Bi_x$ thin films

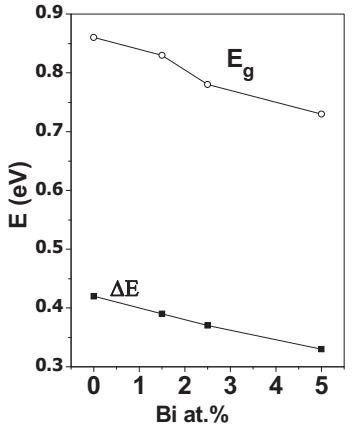

Fig. 5 Plot of E_g and ΔE vs. Bi at. % for $Ge_{20}Te_{80-X}Bi_x$ thin films.

Optical band gap decreases with the addition of Bi content. This behavior is explained on the basis of chemical bond approach (CBA) [28], according to which atoms combine more favorably with atoms of different kind rather than with the same kind and bonds are formed in the sequence of decreasing bond energies until all the available valences are satisfied. Consequently bonds between like atoms will only occur if there is an excess of certain type of atoms. In the above mentioned system, Bi enters into the Ge-Te system and saturates Bi-Te bonds thus decreasing the concentration of Ge-Te bonds. Since the bond energy of Bi-Te bond (125.6 kJ / mol) is lower than that of the Ge-Te bond (156.7 kJ / mol), the average bond energy of the system and hence E_g decreases. Moreover ΔE and E_g are observed to follow similar behavior with Bi at % as shown in Fig. 5. It can be observed that the value of ΔE is less than half of optical band gap *(E_g)* indicating that the Fermi level is not located near the centre of gap.

Table 2. The dc dark conductivity (σ_d), the pre-exponential factor (σ_0), the activation energy for dc conduction (ΔE_d) and optical band gap *(E_g)* for $Ge_{20}Te_{80-X}Bi_x$ thin films.

x	$\sigma_0(dark)\,(\Omega^{-1}cm^{-1})$	$\sigma_d\,(\Omega^{-1}cm^{-1})$	$\Delta E_d\,(eV)$	$E_g\,(eV)$
0	343.78	0.0088	0.28	0.86
1.5	450.34	0.0652	0.23	0.83
2.5	121	0.17	0.18	0.78
5.0	67.31	0.310	0.14	0.73

4. Conclusion

DTA curves of $Ge_{20}Te_{80-X}Bi_x$ (x = 0, 1.5, 2.5, 5.0) glassy alloy are analyzed for T_g, T_c and T_m . T_g as well as T_c are found to increase with increasing Bi content. The results are explained on the basis of coordination number and stiochiometry of the system. T_g is also calculated theoretically and it is found to follow the similar trend as that of experimental values. dc conductivity measurements are carried out on the thin films of the bulk samples and are found to increase with increasing Bi content, whereas the

activation energy *(ΔE)* is found to follow the opposite trend. Optical band gap *(E_g)* is determined by using Tauc extrapolation method and is found to decrease with increasing Bi content. It is also observed that the value of ΔE is less than half of optical band gap *(E_g)* indicating that the Fermi level is not located near the centre of gap.

5. References:

[1] M. Frumar and T. Wagner., Curr. Opin. Solid State Mater. Sci. **7** (2003), 117
[2] A. Znobrik, J. Stetzif, I. Kavich, V. Kavich, V. Osipenko, I. Zachko, N. Balota and O. Jakivchuk, Ukr. Phys. J. **26**, (1981) 212.
[3] J.S. Sanghera and I.D. Aggarwal, J. Non-Cryst. Solids 6 (1999) **656–657**.
[4] K. Schwartz, The Physics of Optical Recording (Springer, Berlin, (1993)
[5] A. Bradley, Optical Storage for Computers Technology and Applications (Ellis Harwood, New York, 1989)
[6] J. Bradangna, S.A. Keneman, in Holographic Recording Media, ed. by H.M. Smith (Springer, Berlin, 1977)
[7] P.A. Thielen, L.B. Shaw, J.S. Sanghera and I.D. Aggarwal, Opt. Express **11** (2003) 3228
[8] J. Troles, F. Smektala, G. Boudebsa, A. Monteila, B. Bureau and J. Lucas, J. Optoelectron. Adv. Mater. **4** (2002) 729
[9] Idem, Appl. Phys. Lett. 49 (1986) 22
[10] T. Takamori, R. Roy and G.J. Mccarthy, Mater. Res. Bull. **5** (1970) 529
[11] S. Lizima, M. Suzi, M. Kikuchi and K. Tanaka, Solid State Commun. **8** (1970) 153
[12] J.A. Savaga, J. Mater. Sci. **6** (1971) 964
[13] J.A. Savaga, J. Non Cryst. Solids **11** (1972) 121
[14] S. Bordas, V.J. Casas, N. Clavaguera and M.T. Clavaguera Mora, Thermochim. Acta **28** (1973) 387
[15] K. Fukui, J. Phy. Soc. Jpn 10 (1992) 1084
[16] I.Kaban, T.Halm, W.Hoyer, P.Jovari and J.Neuefeind: Journal of Non-Crystalline Solids, 120 (2003) **326-327**,
[17] A.K.Varshneya and D.J.Mauro: Journal of Non-Crystalline Solids **353** (2007) 1291
[18] M.Micoulaut, J.C.Phillips: Physical Review B, **67 (**2003) 104204
[19] P.Boolchand, X.Feng and W.J.Bresser: Journal of Non-Crystalline Solids, 348 (2001) **293–295**,
[20] A. Sharma and P.B.Barman, Thin Solid Films 517 (2009) 3020
[21] S.O.Kasap and S.Yannacopoulos: Journal of Materials Research, **4 (**1989), 893
[22] L.Tichy and H.Ticha: Materials Letters, **21 (**1994) 313
[23] L.Tichy and H.Ticha: Journal of Non-Crystalline Solids, **189 (**1995), 141
[24] G. Saffarini, App Phys A 74 (2002) 283-5
[25] N.F. Mott and E.A. Davis, *Electronic Processes in Non-Crystalline Materials*, 2nd edn. (Clarendon, Oxford, 1979)
[26] M. M. Abd El-Raheem, J. Phys.: Condens. Matter 19 (2007) 216209.
[27] J. Tauc, Amorphous and Liquid Semiconductors (New York: Plenum) (1979).
[28] J. Biecerano and S.R.Ovshinesky, J. Non Cryst. Solids 74 (1985) 75.